

3-d resistive MHD simulations of magnetic reconnection and the tearing mode instability in current sheets

G. C. Murphy*

Laboratoire d'Astrophysique de Grenoble, CNRS, Université Joseph Fourier, Grenoble, France

**E-mail: Gareth.Murphy@obs.ujf-grenoble.fr*

R. Ouyed

Department of Physics and Astronomy, University of Calgary, AB, Canada

E-mail: ouyed@phas.ucalgary.ca

G. Pelletier

Laboratoire d'Astrophysique de Grenoble, CNRS, Université Joseph Fourier, Grenoble, France

E-mail: Guy.Pelletier@obs.ujf-grenoble.fr

Magnetic reconnection plays a critical role in many astrophysical processes where high energy emission is observed, e.g. particle acceleration, relativistic accretion powered outflows, pulsar winds and probably in dissipation of Poynting flux in GRBs. The magnetic field acts as a reservoir of energy and can dissipate its energy to thermal and kinetic energy via the tearing mode instability. We have performed 3d nonlinear MHD simulations of the tearing mode instability in a current sheet. Results from a temporal stability analysis in both the linear regime and weakly nonlinear (Rutherford) regime are compared to the numerical simulations. We observe magnetic island formation, island merging and oscillation once the instability has saturated. The growth in the linear regime is exponential in agreement with linear theory. In the second, Rutherford regime the island width grows linearly with time. We find that thermal energy produced in the current sheet strongly dominates the kinetic energy. Finally preliminary analysis indicates a $P(k)$ 4.8 power law for the power spectral density which suggests that the tearing mode vortices play a role in setting up an energy cascade.

Keywords: MHD-Plasma physics-numerical simulations

1. Introduction

Magnetic reconnection plays a critical role in many astrophysical processes, e.g. particle acceleration [1], accretion disks [2] and solar flares [3]. It is also important in laboratory fusion devices such as tokamaks. Magnetic reconnection is a topological change in the field which violates the frozen-flux condition of ideal magnetohydrodynamics (MHD). If a magnetic field can leak across the plasma it can reach a lower energy state - in the case of a current sheet it can undergo “tearing” into filaments or magnetic islands. A current layer of thickness a may dissipate on timescales shorter than the resistive timescale a^2/η due to the tearing mode instability (hereafter TMI). The TMI was first discovered in tokamaks and stellerators and has been extensively studied since the pioneering works [4] and [5] (see also [6], [7], [8]). In this paper we present numerical simulations of the dissipation of current sheets and the formation of magnetic islands due to the tearing mode instability. In Section 2 we remind the reader of the predictions of the linear

and weakly nonlinear analyses of Furth et al. [4] and Rutherford [5]. In Section 3 we present our numerical method. In Section 4 we compare the results with linear and weakly nonlinear theory. In Section 5 we present power spectra derived from 3d simulations. In Section 6 we discuss the pitfalls of simulations where reconnection is not properly tracked and the implications for reconnection-driven turbulence.

2. Theory

2.1. The linear regime

In the linear analysis it is assumed that resistivity is only important within the current layer. Separate solutions may then be derived for the exterior, ideal MHD region and the interior, resistive region. Using asymptotic matching [4] derived stability range and growth rates for the TMI in the inviscid linear regime, neglecting the effects of compressibility. The range of the instability is $\alpha < 1, \alpha = ak$, where k is the wave number and a is the current sheet width.

The growth rate is:

$$\gamma \sim \alpha^{-\frac{2}{5}} S^{\frac{2}{5}} / \tau_R \quad (1)$$

The linear growth rate is a function of the mode number, k , the current sheet width, a , and the Lundquist or magnetic Reynolds number, S . The equations are valid for $\alpha > S^{-\frac{1}{4}}$. The system stays linear for as long as the magnetic island does not exceed the width of the current sheet.

2.2. Non-linear regime

Rutherford [5] studied the evolution of the TMI in the weakly nonlinear regime, by considering the effect of second order eddy currents on the current sheet. [5] found in the nonlinear regime that the island width grows as t , instability growth rate slows down from exponential to t^2 , and that the critical amplitude where the linear solution ceases to be valid is:

$$B_{max} = \frac{\sqrt{2\eta\rho\gamma}}{\alpha} \quad (2)$$

Table 1. Growth Rates and Saturation Times for Lundquist number 2400

α	Linear Growth Rate [τ_A^{-1}]		Saturation [τ_A]	
	Theory	Sim	Theory	Sim
0.01	0.0590	0.0528	153.233	170
0.04	0.0339	0.0484	394.980	250
0.3	0.0151	0.01276	508.370	520

2.3. Previous work

More recent work has concentrated on including the physics of the Hall effect using multifluid or Hall MHD and electron inertia, using PIC techniques. Significant increase in reconnection rates is found in these studies [9]. However in these works the authors do not compare against analytical theory nor is the 3D power spectrum calculated.

3. Numerical setup

We perform first 2D and then 3D simulations in resistive MHD using the astrophysical code PLUTO.

As in any numerical code some numerical resistivity is present. In the linear analysis numerical resistivity has been assumed to be small in comparison with the physical resistivity. Our initial mean field is

a Harris current sheet of the form $B_y = \tanh(x)$. We initialise the field in the magnetic vector potential $A_z = \ln|\cosh(x)|$ and take the curl to derive \mathbf{B} . To this we add a perturbation of the form $\cos(kx)$ in 2d and $\cos(kx)\cos(ky)$ in 3d. Free parameters are α , $\beta = \frac{\nu}{B^2}$ and the resistivity η . Zero-gradient Neumann-like ‘‘outflow’’ boundary conditions often produce subsonic reflection for compressible flows [10, 11]. We use a coarse mesh boundary which reduces this effect.

4. Simulation Results

4.1. 2D

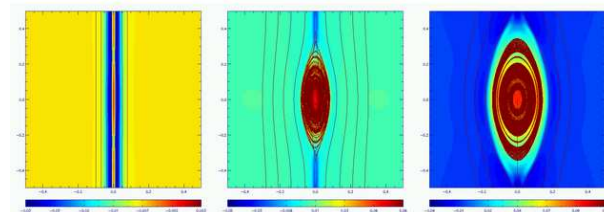


Fig. 1. Formation of magnetic islands: magnetic field lines and density colourmap are shown at times: 245, 365, 490.

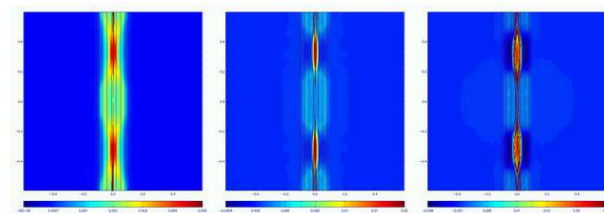


Fig. 2. Same as Figure 1 but for $\alpha = 0.3$

We performed 2d and 3d simulations of current sheets for different initial perturbations $k = 0.01, 0.04, 0.3, 0.6$. We tracked the growth rate of the cross-sheet magnetic field B_x . In the simulations an initial transient period, $t_{transient} \sim 100\tau_A$ roughly corresponding to half the crossing time of the domain ($t = 112\tau_A$) was observed before the linear mode was established. As the tearing mode grows linearly, field lines reconnect, new separatrices are formed and magnetic islands grow in size, eventually exceeding the size of the original current sheet. In Figures 1 and 2 the time evolution of magnetic islands for $\alpha = 0.01, 0.3$ are plotted against time in

units of the Alfvén crossing time, τ_A .

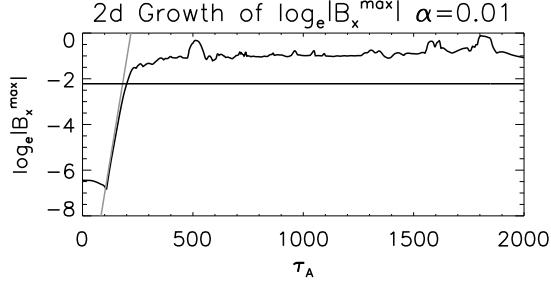


Fig. 3. Growth of log of maximum B_x plotted against time. The linear growth rate is plotted and the critical value for saturation.

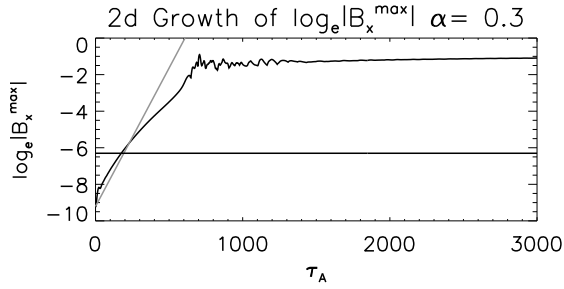


Fig. 4. Same as Fig. 3 but for $\alpha = 0.3$.

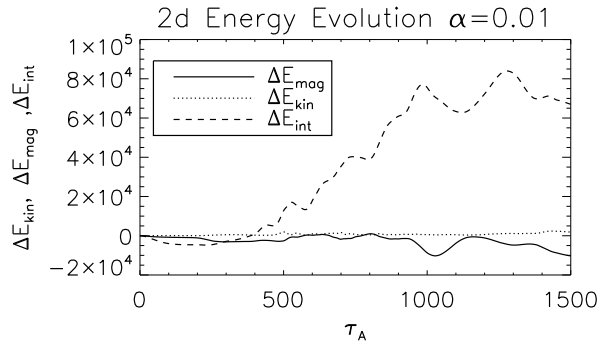


Fig. 5. Time evolution of change in kinetic energy, magnetic energy and internal energy. Most of the magnetic energy is converted into thermal energy.

4.1.1. Agreement with linear analysis

In Figures 3 and 4 the growth rate in cross-sheet magnetic field, B_x for different exciting modes of the TMI is plotted against time. In all cases a lin-

ear regime is found with slopes near the analytical predictions of Furth et al. [4].

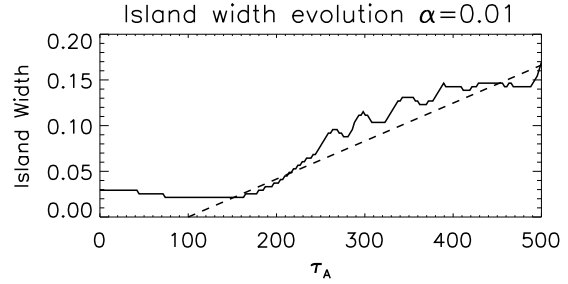


Fig. 6. Magnetic island width evolution plotted against time in units of τ_A for $\alpha = 0.01$. The width is estimated using the full-width half maximum of the thermal pressure. It remains approximately constant in the linear phase and transfers to a linear growth in t once in the Rutherford regime.

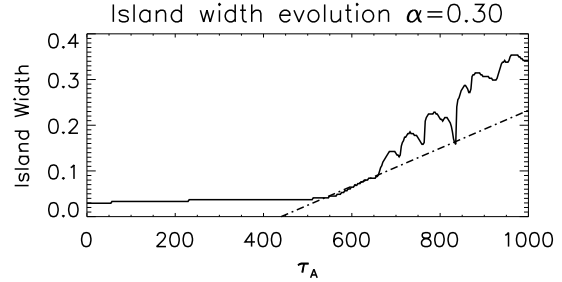


Fig. 7. Same as 6 but for $\alpha = 0.3$.

4.1.2. Agreement with nonlinear analysis

We find plotting the island width against time that it remains small in the linear regime and grows as t^2 in the Rutherford regime. We can estimate the time of transition from linear to Rutherford from both the B_x plots and the island width plots, however the island width plots provide a more accurate estimate. The time at which the system becomes nonlinear is tabulated in Table 1. The magnetic island width can be derived from eqn 18. in [5, 6] and can be written in approximate form as

$$w_I \sim \frac{\tilde{t} - t_d}{S}, \quad (3)$$

where t_d accounts for the total delay (transient and time spent in linear regime) in our simulations before entering the Rutherford regime.

5. 3D Power spectra

In Figure 8 we plot the power spectrum for $\beta = 2$ 3d current sheet. The slope of $P(k)$ is -4.8 , within the range of values found by [12] for $\beta = 1$ and $\beta = \infty$. [12] note that in their driven, supersonic turbulence simulation they have a constant beta and a constant mass-to-flux ratio “modulo the numerical reconnection effect”. We obtain the same power spectrum scaling without any added velocity perturbations.

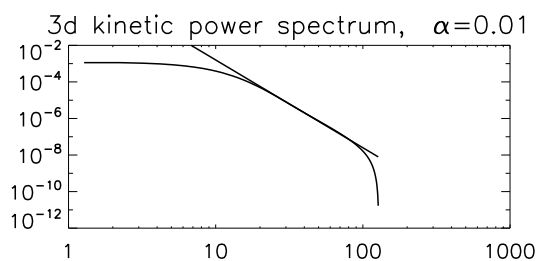


Fig. 8. 3d kinetic power spectrum at time $t = 295\tau_A$ with overplotted $k^{-4.8}$

6. Discussion and Conclusion

6.1. Consequences for driven-turbulence simulations

Our results show that even without either a driven turbulence mechanism, or an initially turbulent velocity spectrum it is possible for the vortices generated by the TMI to mimic the power spectrum seen in simulations of turbulence. This can have serious consequences for MHD simulations where the resistivity is not explicitly constrained (i.e. numerical resistivity plays a role), since there will be inevitably be some numerical-reconnection driven vortices present in the simulation. However using an explicit resistivity, the contribution from reconnection can be estimated using the formulae in [4, 5].

Finally, we propose as a benchmark for resistive MHD codes the tearing mode instability test, which can be compared with both analytical results for both the linear and nonlinear regimes, as well

as with laboratory experiments. The test may also prove useful as a way of quantifying the effects of numerical resistivity in an MHD code.

Acknowledgements

G.C.M. would like to acknowledge funding from the Agence Nationale de Recherche, the University of Calgary, and the Dublin Institute for Advanced Studies.

References

- [1] T. D. Phan, J. T. Gosling, M. S. Davis, R. M. Skoug, M. Øieroset, R. P. Lin, R. P. Lepping, D. J. McComas, C. W. Smith, H. Reme and A. Balogh, *Nature* **439**, 175(January 2006).
- [2] J. F. Hawley and S. A. Balbus, *ApJ* **376**, 223(July 1991).
- [3] K. Shibata, Evidence of Magnetic Reconnection in Solar Flares and a Unified Model of Flares, in *Structure Formation and Function of Gaseous, Biological and Strongly Coupled Plasmas*, p. 74, September 1999.
- [4] H. P. Furth, J. Killeen and M. N. Rosenbluth, *Physics of Fluids* **6**, 459 (1963).
- [5] P. H. Rutherford, *Physics of Fluids* **16**, 1903(November 1973).
- [6] R. B. White, *Reviews of Modern Physics* **58**, 183(January 1986).
- [7] E. Priest and T. Forbes, *Magnetic Reconnection* (Magnetic Reconnection, by Eric Priest and Terry Forbes, pp. 612. ISBN 0521481791. Cambridge, UK: Cambridge University Press, June 2000., June 2000).
- [8] D. Biskamp, *Magnetic Reconnection in Plasmas* (Magnetic reconnection in plasmas, Cambridge, UK: Cambridge University Press, 2000 xiv, 387 p. Cambridge monographs on plasma physics, vol. 3, ISBN 0521582881, November 2000).
- [9] J. Birn, J. F. Drake, M. A. Shay, B. N. Rogers, R. E. Denton, M. Hesse, M. Kuznetsova, Z. W. Ma, A. Bhattacharjee, A. Otto and P. L. Pritchett, *J. Geophys. Res.* **106**, 3715(March 2001).
- [10] P. J. Roache, *Computational Fluid Dynamics* (Computational Fluid Dynamics, Albuquerque: Hermosa, 1976, 1976).
- [11] T. Colonius, *Ann. Rev. Fluid. Mech.* **36**, 315(June 2004).
- [12] J. G. Vestuto, E. C. Ostriker and J. M. Stone, *ApJ* **590**, 858(June 2003).